



# INVESTIGATIONS ON THE MECHANICAL AND ELECTRICAL PROPERTIES OF AN L-CYSTEINE NICOTINAMIDE MONOHYDRATE SINGLE CRYSTAL

V. AZEEZAA<sup>\*</sup>, T. G. SUNITHA<sup>a</sup>,  
A. JOSEPH ARUL PRAGASAM<sup>b</sup> and S. SURESH<sup>c</sup>

Department of Physics, SRR Engineering College, CHENNAI – 603103 (T.N.) INDIA

<sup>a</sup>Department of Chemistry, Pachaiyappa's College, CHENNAI – 600030 (T.N.) INDIA

<sup>b</sup>Department of Physics, Sathyabama University, CHENNAI – 600119 (T.N.) INDIA

<sup>c</sup>Department of Physics, AMET University, Kanathur, CHENNAI – 600123 (T.N.) INDIA

## ABSTRACT

Single crystal of L-Cysteine Nicotinamide Monohydrate (LCNM) was grown by slow evaporation method. Single crystal XRD method was used for structural identification. The microhardness study shows that the hardness steadily increases with increase in loads. Work hardening coefficient indicates that the grown crystals are moderately softer. Variation of stiffness constant with load for the given crystals was analysed. Dielectric constant and dielectric loss have been obtained as a function of frequency between 50 Hz -5 MHz and different temperatures. The dependence of AC conductivity ( $\sigma_{ac}$ ) on temperature and frequency of the applied field (50 Hz–5 MHz) was studied. The D.C. conductivity was deduced from the A. C. conductivity and activation energy is calculated. The photoconductivity studies reveal that the LCNM crystal exhibits negative photoconductivity nature of the grown single crystal.

**Key words:** Single crystal, Microhardness, Dielectric loss, Dielectric constant, AC and DC conductivity, Photoconductivity.

## INTRODUCTION

A non-linear optical (NLO) frequency conversion material is of vital role in the field of photonics and optoelectronics applications. NLO crystals are not only confined because of their NLO properties. They also study other characteristics such as hardness and dielectric,

---

\* Author for correspondence; E-mail: azeezaaphysics@gmail.com

as these will determine technological utility of developed materials<sup>1</sup>. Organic materials have drawn the attention of material scientists because of their piezoelectric, pyroelectric, non-linear optics and electro-optical applications<sup>2</sup>. Materials with large second-order optical nonlinearities, short transparency cut-off wavelengths and stable physicochemical performances are needed in order to realize many of these applications<sup>3</sup>. The mechanical and dielectric properties of an organic material, nicotinamide<sup>4</sup> and L-Cysteine hydrochloride monohydrate<sup>5</sup> was reported earlier. In the present work, we report the growth of non-linear organic crystal L-Cysteine nicotinamide monohydrate (LCNM) by slow evaporation technique. From single crystal X-ray diffraction studies carried out, it was found that the LCNM crystal had its monoclinic structure with lattice parameters  $a = 7.21 \text{ \AA}$ ,  $b = 6.72 \text{ \AA}$ ,  $c = 7.54 \text{ \AA}$ ,  $V = 365 \text{ \AA}^3$ ,  $\beta = 99.47^\circ$ .

## EXPERIMENTAL

### Material synthesis

LCNM was synthesized using L-Cysteine and nicotinamide in a stoichiometric ratio 2:1 in the presence of HCl. The required amount of L-Cysteine and nicotinamide were estimated from the following reactions shown in Fig. 1. The calculated amount of salts were first dissolved in double distilled water and then acidified with HCl. The solution was agitated with a magnetic stirring device at 35°C to yield homogeneous mixture of solution and filtered after complete dissolution of the starting materials.

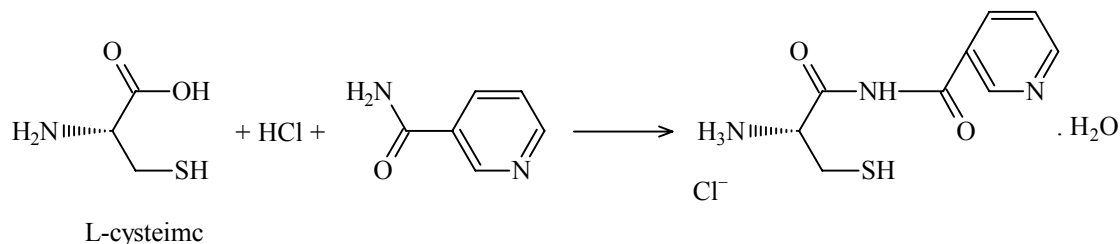


**Fig. 1: Reaction of LCNM**

### Crystal growth

Single crystals of LCNM were grown from saturated solution by slow evaporation of the solvent at room temperature. The good quality seed was suspended in super saturated solution and the solution was slowly cooled at a cooling rate of 0.05°C per day at 35°C. After growth period of 25 to 30 days good transparent crystal to a size of about  $29 \times 7 \times 5 \text{ mm}^3$  was harvested. Fig. 2 shows the photograph of LCNM crystal.

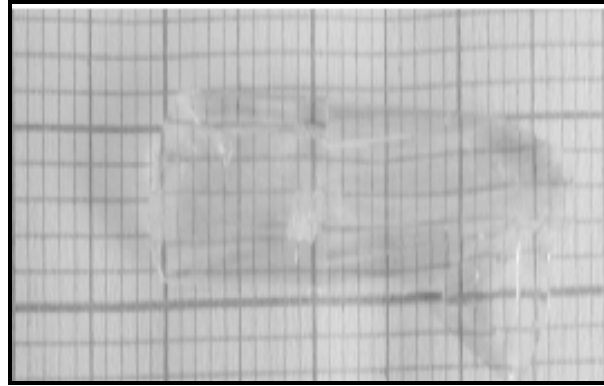


**Fig. 2: Photograph of LCNM single crystal**

## RESULTS AND DISCUSSION

### Microhardness test

Microhardness testing is one of the best methods of understanding the mechanical properties of material such as fracture behaviour, yield strength, brittleness index and temperature of cracking. The hardness is generally measured as the ratio of applied load to the surface area of the indentation. Microhardness studies were carried out on the polished LCNM crystal using Matsuzawa, MMT-X7B Vickers microhardness tester fitted with a diamond indenter. The well-polished LCNM crystal with smooth and dominant face was placed on the platform on the Vickers microhardness tester. The crystal was indented gently by the loads varying from 1 g to 50 g for a dwell period of 10s using Vickers diamond pyramid indenter attached to an incident ray research microscope. Vickers hardness number was determined using the relation<sup>6</sup>.

$$H_V = 1.8544 P/d^2 \text{ Kg/mm}^2 \quad \dots(1)$$

A graph between  $H_V$  and load  $P$  was shown in Fig. 3a. From the graph, it was observed that  $H_V$  increase with load  $P$  for the grown crystal. This phenomenon is known as reverse indentation size effect<sup>7-9</sup>. When the material is deformed by the indenter, dislocations are generated near the indentation site. The major contribution to the increase in hardness is attributed to the high stress required for homogenous nucleation of dislocations in the small dislocation-free region indented<sup>10</sup>. The reverse indentation size effect can be caused by the relative predominance of nucleation and multiplication of dislocations. The other reason for reverse indentation size effect is that the relative predominance of the activity of either two sets of slips planes of a particular slip system or two slip systems below and above a particular load<sup>11</sup>. The reverse indentation size effect phenomenon essentially takes place in

crystals, which readily undergo plastic deformation<sup>12</sup>. The relation between load and the size of indentation can be interpreted using Meyer's law:

$$P = K_1 d^n \quad \dots(2)$$

Where  $k_1$  is the standard hardness and  $n$  is the Meyer's number index. The slope of  $\log P$  versus  $\log d$  gives the value of  $n$  and it is estimated to be 2.27 and from the intercept the value of  $k_1$  is found to be 1.02, which is shown in Fig. 3b. According to Onitsch<sup>13</sup> and Hanneman<sup>14</sup>,  $n$  should be between 1 and 1.6 for hard materials and above 1.6 for softer ones. Thus LCNM crystal belongs to soft material category. Meyer number is a measure of the indentation size effect. The elastic stiffness constant ( $C_{11}$ ) gives an idea about tightness of bonding between neighbouring atoms. The stiffness constant for different loads has also been calculated using Wooster's empirical formula<sup>15</sup>.

$$C_{11} = H_V^{7/4} \quad \dots(3)$$

The stiffness constant increases with increase of loads as shown in Fig. 3c. High value of  $C_{11}$  indicates that the binding forces between the ions are quite strong<sup>16</sup>.

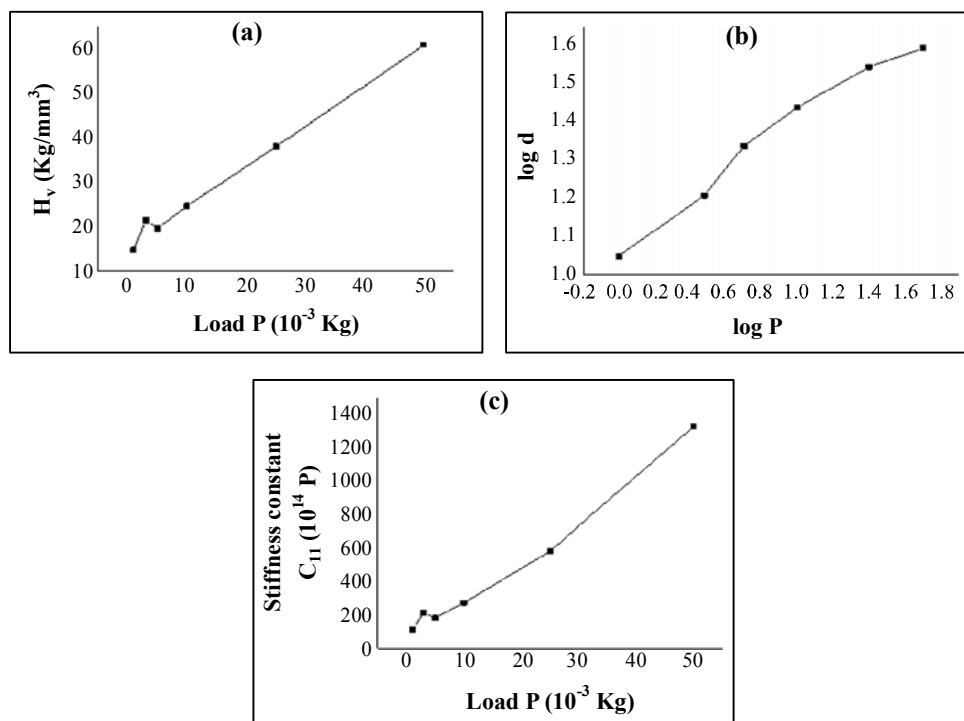


**Fig. 3: (a)  $H_V$  Vs Load P (b)  $\log P$  Vs  $\log d$  (c) Load P Vs  $C_{11}$  of LCNM crystal**

## Dielectric measurement

A study of the dielectric properties provides information about electric fields within the solid materials. Frequency dependence of these properties gives a great insight into the materials applications. Dielectric properties are correlated with electro-optic property of the crystals: particularly when they are non-conducting materials<sup>17</sup>. Microelectronic industries need low dielectric constant  $\epsilon_r$  materials as an interlayer dielectric<sup>18</sup>. LCNM crystal cut in the appropriate dimension was subjected to dielectric measurements. A rectangular shape of approximate thickness of 0.6 mm and area of cross section of 13.65 mm<sup>2</sup> crystal was subjected to dielectric studies. Silver paste was coated on both the surfaces of the crystal to make a firm contact between the crystal and the copper electrodes. The capacitance and dissipation factor of the parallel plate capacitors formed by the copper plate and electrodes having the crystal as was measured using HIOKI 3532 LCR HITESTER. The studies were carried from 40°C to 100°C for a frequency varying from 50 Hz to 5 MHz. The variation of dielectric constant with log frequency is shown in Fig. 4. The dielectric constant was calculated using the formula,

$$\epsilon_r = \frac{Ct}{\epsilon_0 A} \quad \dots(4)$$

Where C is the capacitance (F), t the thickness (m), A the cross-sectional area (m<sup>2</sup>) of the sample and  $\epsilon_0$  is the absolute permittivity of the free space having a value of  $8.854 \times 10^{-12} \text{ Fm}^{-1}$ . The imaginary dielectric constant  $\epsilon_r'$  of the capacitor was calculated using the relation.

$$\epsilon_r' = \epsilon_r \tan \delta \quad \dots(5)$$

where  $\tan \delta$  is the loss tangent. The dielectric constant  $\epsilon_r$  obtained for LCNM was higher at lower frequencies and then it was found to decrease with the increasing frequencies and saturated for further increase in the frequency which could be attributed to space charge polarization mechanism of molecular dipoles<sup>19</sup>. The electronic exchange of a number of ions in the crystals gives local displacement of electrons in the direction of the applied field, which in turn gives rise to polarization. Crystals with high dielectric constant lead to more power dissipation and hence at higher frequencies, the power dissipation in the crystal may have lower value<sup>20-23</sup>. Fig. 5 shows the variation of dielectric loss with log frequency. From the figure it is observed that the dielectric loss decreases with increase in frequency at different temperatures. As the frequency increases, the dielectric constant decreases. Thus, LCNM crystal having low value of dielectric constant is suitable for the enhancement of SHG coefficient<sup>24</sup>.

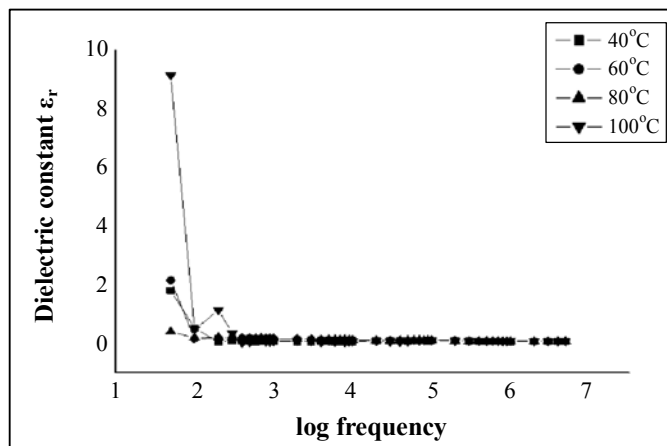


Fig. 4: log Frequency Vs dielectric constant of LCNM crystal

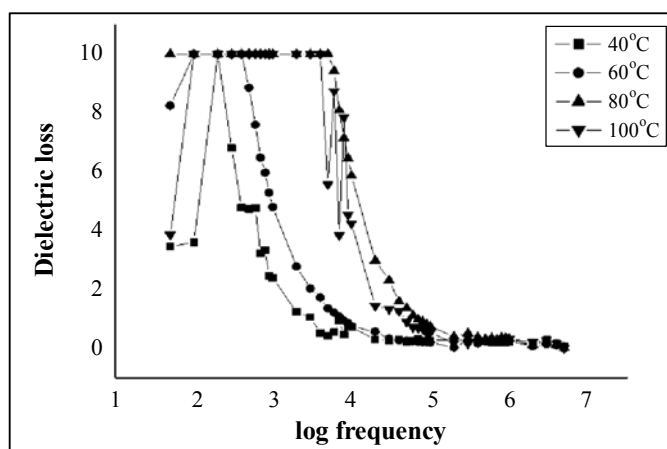


Fig. 5: log Frequency Vs dielectric loss of LCNM crystal

### AC conductivity study

The alternating current conductivity of the LCNM crystal was calculated using the relation.

$$\sigma_{ac} = \omega \epsilon_0 \epsilon_r \tan \delta \quad \dots(6)$$

Where  $\omega$  is the angular frequency of the applied ac field in Hz. In the high temperature intrinsic region, the effect of impurity on electrical conduction had not made any appreciable change whereas in the low temperature extrinsic region, the presence of impurity in the crystal had an impact and particularly increases its conductivity. The

presence of impurities and vacancies predominantly determine this region. The energy needed to form the defect was larger than the energy needed for its drift. The activation energy of the crystal was calculated from an Arrhenius plot using the relation<sup>25</sup>.

$$\sigma_{ac} = \sigma_o \exp(-E_{ac}/kT) \quad \dots(7)$$

Where  $\sigma_{ac}$  is the conductivity at temperature T,  $E_{ac}$  the activation energy for the electrical process and k is the Boltzmann constant. The behaviour of AC conductivity with frequency ranging from 50 Hz to 5 MHz at various temperatures is shown in Fig. 6. The value of the activation energy was calculated from the slope of the graph between  $\sigma_{ac}$  versus log frequency and was found to be 0.0295 eV.

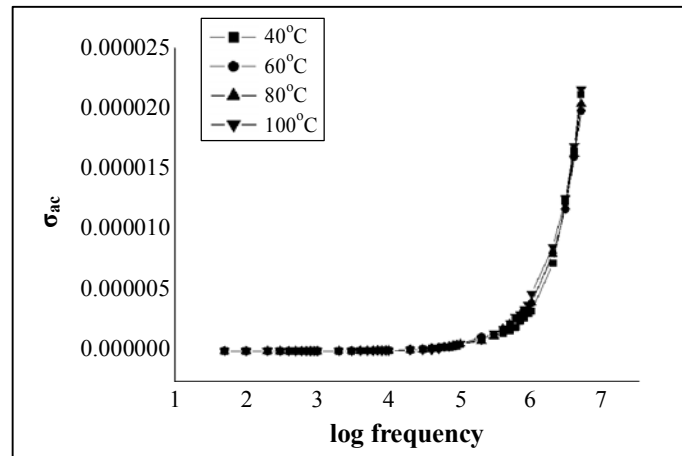


**Fig. 6: log Frequency Vs  $\sigma_{ac}$  of LCNM crystal**

### DC conductivity study

The direct current conductivity measurements were carried out using the conventional two-probe technique at various temperatures ranging from 40°C to 100°C<sup>26</sup>. The resistance of the crystal was measured using a million megohmmeter. The crystal was perfectly cut into rectangular shape and then polished using silicon carbide paper. The DC conductivity of LCNM crystal was calculated using the relation<sup>27</sup>,

$$\sigma_{dc} = \frac{d}{RA} \quad \dots(8)$$

Where R is the resistance measured, d is the thickness of the sample and A is the area of face in contact with the electrode. The  $\sigma_{dc}$  values were fitted into the equation,

$$\sigma_{dc} = \sigma_o \exp(-E_{dc}/kT) \quad \dots(9)$$

Fig. 7 shows the variation of  $\sigma_{dc}$  and log frequency, which represents the temperature dependence of conductivity of the crystal and the conductivity was found to increase with increase in temperature for LCNM crystal. Electrical conductivity depends on thermal treatment of crystal<sup>28</sup>. The DC activation energy  $E_{dc}$  of the LCNM crystal was found to be 0.059 eV.

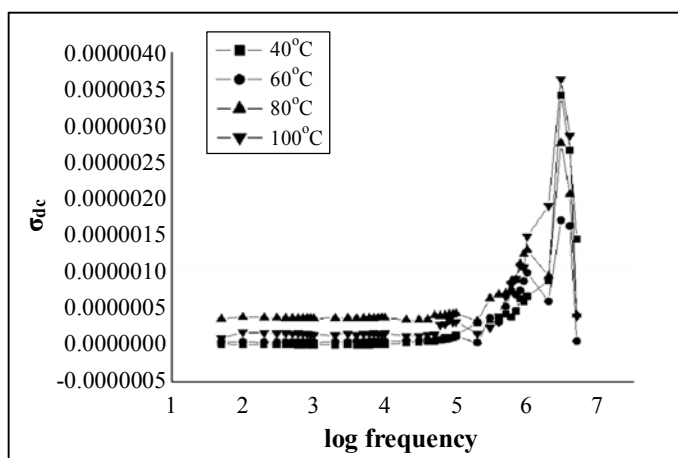


**Fig.7: log Frequency vs  $\sigma_{dc}$  of LCNM crystal**

### Photoconductivity studies

Photoconductivity is an important property of solids by means of which the bulk conductivity of the sample changes due to incident radiation, which include the generation and recombination of charge carriers and their transport to the electrodes. It also provides valuable information about physical properties of materials and offers applications in photo detection and radiation measurements. A polished sample of LCNM crystal is attached to a microscopic slide. Thin copper wires (0.14 cm diameter) are fixed at a distance of 0.1 cm on the sample by silver paint. The sample is then connected in series to a DC power supply and a picoammeter (keithley 480). On keeping the crystal in the same experimental setup, the crystal is illuminated with the radiation from a halogen lamp (100 w) containing iodine vapour and tungsten filament, by focusing a spot of light on it with the help of a convex lens. Fig. 8 shows the variation of both dark current ( $I_d$ ) and photocurrent ( $I_p$ ) with applied field. It is seen from the plots that both  $I_d$  and  $I_p$  of the crystal increase linearly with applied field. It is observed from the plot that the dark current is always higher than the photo current, thus confirming the negative photoconductivity nature of the single crystal. However, the



negative photoconductivity in this case may be due to the reduction in the number of charge carriers or their lifetime in the presence of radiation<sup>29-31</sup>. Decrease in lifetime with illumination could be due to the trapping process and increase in carrier velocity according to the relation<sup>32</sup>.

$$\tau = (vsN)^{-1} \quad \dots(10)$$

Where  $v$  is the thermal velocity of the carriers,  $s$  is the capture cross-section of the recombination centres and  $N$  is the carrier concentration. As intense light falls on the sample, the lifetime decreases. In the Stockman model, a two level scheme is proposed to explain negative photoconductivity<sup>33</sup>. As a result, the recombination of electrons and holes take place resulting in decrease in the number of mobile charge carriers, giving rise to negative photoconductivity.

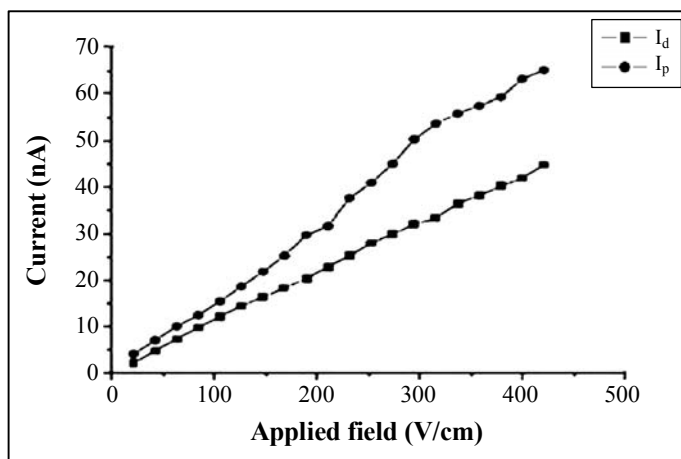


**Fig. 8: Field dependent photoconductivity of LCNM crystal**

## CONCLUSION

Single crystals of L-Cysteine Nicotinamide Monohydrate (LCNM) have been grown by slow evaporation method. Microhardness test on this crystal reveals that the LCNM belongs to soft category. Dielectric constant and dielectric loss of the crystal is found to decrease with increase in frequency higher values of dielectric constant occurs at higher temperature. The activation energy was calculated from the slope of the plot of AC/DC conductivity. The photocurrent was less than the dark current, signifying negative photoconducting nature. The encouraging electrical properties of the crystal indicate the suitability of this crystal for photonics device fabrication.

## REFERENCES

1. N. J. Long, *Angew. Chem. Int. Ed. Engl.*, **34**, 21-38 (1995).
2. D. S. Chemla and J. Zyss, Academic Press, New York (1987).
3. X. Q. Wang, D. Xu, M. K. Lu, D. T. Yuan, J. Huang, S. G. Li, G. W. Lu, H. Q. Sun, S. Y. Guo, G. H. Zhang, X. L. Duan, H. Y. Liu and W. L. Liu, *J. Cryst. Growth*, **247**, 432-437 (2003).
4. P. Ramesh Kumar, R. Gunaseelan, S. Kumararaman, G. Baghavannarayana and P. Sagayaraj, *Physica B: Condensed Matter.*, **125**, 15-19 (2011).
5. M. Loganayaki and P. Murugakoothan, *Asian J. Chem.*, **23(10)**, 5085-5088 (2011).
6. B. W. Mott, *Microindentation Hardness Testing*, Butterworths, London (1956).
7. L. Zhao, S. B. Li, G. A. Wen, B. Peng and W. Huang, *Mater. Chem. Phys.*, **100(2-3)**, 460-463 (2006).
8. S. Boomadevi, H. P. Mittal and R. Dhanasekaran, *J. Cryst. Growth*, **261(1)**, 55-62 (2004).
9. S. Karan and S. P. S. Gupta, *Mater. Sci. Eng, A.*, **398(1-2)**, 198-203 (2005).
10. A. G. Kunjomana and K. A. Chandrasekharan, *Cryst. Res. Technol.*, **40**, 782-785 (2005).
11. K. Sangwal, *Mater. Chem. Phys.*, **63**, 145-152 (2000).
12. H. Li, Y. H. Han and R. C. Bradt, *J. Mater. Sci.*, **29**, 5641-5645 (1994).
13. E. M. Onitsch, *Mikroskopie.*, **2**, 131-134 (1947).
14. M. Hanneman, *Metall. Manch.*, **23**, 135-139 (1941).
15. W. A. Wooster, *Rep. Prog. Phys.*, **16**, 62-82 (1953).
16. P. Ashok Kumar, R. Ezhil Vizhi, N. Vijayan and D. Rajan Babu, *Sch. Res. Lib.*, **2**, 247-254 (2010).
17. S. Boomadevi, H. P. Mittal and R. Dhanasekaran, *J. Cryst. Growth*, **261**, 55-62 (2004).
18. B. T. Hatton, K. Landskron, W. J. Hunks, M. R. Bennett, D. D. Perovic, G. A Ozinna, *Mater. Today*, **9(3)**, 22-31 (2006).
19. L. R. Dalton, *J. Phys. Cond. Matter.*, **15**, R897-R934 (2003).
20. R. H. Bube, *Photoconductivity of Solids*, John Wiley and Sons, Inc., New York (1960).

21. C.-Y. Chung, Y.-H. Chang, G.-J. Chen and Y.-L. Chai, *J. Cryst. Growth*, **284(1-2)**, 100-107 (2005).
22. K. V. Rao and A. Smakula, *J. Appl. Phys.*, **36(6)**, 2031-2038 (1965).
23. K. V. Rao and A. Smakula, *J. Appl. Phys.*, **37(1)**, 319-323 (1966).
24. R. C. Miller, *Appl. Phys. Lett.*, **5**, 17-19 (1964).
25. B. Lal, K. K. Bamzai, P. N. Kotru and B. M. Wanklyn, *Mater. Chem. Phys.*, **85**, 353-365 (2004).
26. S. Suresh and P. Mani, *Inter. J. Scient. Engg. Res.*, **3**, 1-5 (2012).
27. S. Perumal and C. K. Mahadevan, *Physica B: Physics of Condensed Matter.*, **367(1-4)**, 172-181 (2005).
28. I. Bunget and M. Popescu, *Physics of Solid Dielectrics*, Elsevier, New York (1984).
29. B. F. Levine, C. G. Bethra, C. D. Thurmond, R. T. Lynels and J. L. Bernstein, *J. Appl. Phys.*, **50(4)**, 2523-2527 (1979).
30. R. H. Bube, *Photoconductivity of Solids*, Wiley, New York (1981).
31. I. M. Ashraf, H. A. Elshaik and A. M. Badr, *Crystal Res. Tech.*, **39(1)**, 63-70 (2004).
32. P. Koteeswari, P. Mani and S. Suresh, *J. Cryst. Process and Techn.*, **2**, 117-120 (2012).
33. V. N. Joshi, *Photoconductivity*, Marcel Dekker, New York (1990).

*Revised : 15.07.2015*

*Accepted : 17.07.2015*